Insect science

Insect Science (2025) 0, 1–16, DOI 10.1111/1744-7917.70087

ORIGINAL ARTICLE

The role of dopaminergic neuronal clusters in governing division of labor in ants

Wenjiang Zhong[1,2], Nianxia Xie[3,4], Guo Ding[5], Jie Zhao[1], Pei Zhang[4,6], Qiye Li[4,6], Hao Ran[1], Guojie Zhang[5,7] and Weiwei Liu[1,8]

[1]*State Key Laboratory of Genetic Evolution & Animal Models, Kunming Institute of Zoology, Chinese Academy of Sciences, Kunming, China;* [2]*Kunming College of Life Science, University of Chinese Academy of Sciences, Kunming, China;* [3]*College of Life Sciences, University of Chinese Academy of Sciences, Beijing, China;* [4]*BGI Research, Wuhan, China;* [5]*Center of Evolutionary & Organismal Biology, Women's Hospital at Zhejiang University School of Medicine, Hangzhou, China;* [6]*State Key Laboratory of Genome and Multi-omics Technologies, BGI Research, Shenzhen, China;* [7]*Liangzhu Laboratory, Zhejiang University Medical Center, Hangzhou, China and* [8]*Yunnan Key Laboratory of Biodiversity Information, Kunming, China*

Abstract Reproductive division of labor is one of the most prominent features of social insects. Yet, the neural mechanisms that govern this division and the associated behavioral differentiation among castes remain obscure. In this study, we systematically characterized the anatomical features of dopamine neurons in the brain of *Monomorium pharaonis* and compared the cell number and spatial distribution of these neurons across castes. We identified 17 anatomically distinct clusters of dopamine neurons in the ant brain, with cell numbers varying from ~322 to ~431 across castes. The major dopamine clusters are located in brain regions analogous to those in flies, with 2 clusters, PAL and PPL1 exhibiting significantly higher cell numbers in ants than in flies. Notably, 4 clusters, DAM, D1, DPL, and PPL2, showed remarkable variation in cell numbers across castes. Using single-cell transcriptomics, we identified specific molecular markers for subdividing dopamine neurons. We validated the expression of multiple neuropeptide genes in specific dopamine clusters. In particular, we found that PPL2 cluster can be further divided into 2 subclusters, PPL2a and PPL2b, which are partially labeled by the peptide gene *Nplp1*. PPL2b neurons, characterized by larger cell bodies, and present only in unmated queens and males, are absent in mature queens and workers. These neurons are located adjacent to *Nlg2*-expressing lobular neurons, which are also absent in workers and may play a role in regulating mating behaviors. Our findings provide a foundation for further investigation into the neural mechanism underlying division of labor and caste-specific behaviors in ant.

Key words ant superorganism; brain; comparative anatomy; division of labor; dopamine; neural mechanism

Introduction

The emergence of social organization is a key milestone in the evolution of life (Szathmáry & Smith, 1995). Ants have achieved remarkable evolutionary and ecological success, primarily due to their division of labor and advanced social organization (Hölldobler & Wilson, 1990). This division of roles and responsibilities across castes underscores the intricate social organization of

Correspondence: Weiwei Liu, State Key Laboratory of Genetic Evolution &Animal Models, Kunming Institute of Zoology, Chinese Academy of Sciences, Kunming 650201, China. Tel: +86 15887168375; email: liuweiwei@mail.kiz.ac.cn. Guojie Zhang, Center of Evolutionary & Organismal Biology, and Women's Hospital at Zhejiang University School of Medicine, Hangzhou, China. Email: guojiezhang@zju.edu.cn

ant colonies. Therefore, as early as 1910, William Morton Wheeler was the first to propose the superorganism concept for ant colonies, drawing an analogy between the queen-worker caste differentiation within the ant colony and the germ-soma cellular differentiation in Metazoan organisms. In this analogy, the queen functions as the colony's germline, while workers act as its soma (Wheeler, 1910; 1911). Wheeler's concept has been further supported by a recent study that provided a detailed molecular mechanism for the development of superorganisms (Qiu *et al.*, 2022).

The mechanisms by which the specialized behaviors of distinct ant castes are governed by their brains, as well as how these brains are developmentally differentiated remain poorly understood. A wealth of studies has identified genetic, epigenetic, environmental, nutritional, and hormonal regulators that interact intricately to shape the formation, function, and plasticity of neural circuits, ultimately influencing behaviors related to different castes (Schwander *et al.*, 2008; Bonasio *et al.*, 2010; Simola *et al.*, 2016; Gospocic *et al.*, 2017; Chandra *et al.*, 2018; Libbrecht *et al.*, 2018; Opachaloemphan *et al.*, 2018; Qiu *et al.*, 2018; Rajakumar *et al.*, 2018; Qiu *et al.*, 2022; Goolsby *et al.*, 2024; Li *et al.*, 2024; Liu & Li, 2024). And differences in neurochemical features, such as whole-brain levels of biogenic amines, are found to be associated with distinct social roles in ants. In *Acromyrmex echinatior* workers, foragers had higher levels of dopamine and octopamine compared to workers that perform waste management tasks (Smith *et al.*, 2013). In *Oecophylla smaragdina*, major workers had higher octopamine levels which is positively correlated with their higher territorial defense behavior (Kamhi *et al.*, 2015).In addition to variations in neurochemical activity and gene expression, differential investments in brain neuropil are also closely associated with task specialization in ants (Muscedere & Traniello, 2012; Gordon *et al.*, 2019; Arganda *et al.*, 2020; Li *et al.*, 2022; Muratore *et al.*, 2022). By comparing the relative sizes of brain compartments, many studies suggest that mosaic alterations of brain composition contribute to division of labor. For examples, in *Monomorium*, *Pheidole*, *Atta*, and *Cephalotes* ants, distinct brain structures—such as optic lobes, antennal lobes, mushroom bodies, subesophageal zones, and other brain regions—vary significantly across castes, age groups, and species. These structural differences collectively enable ant colonies to function as complementary and integrated superorganisms, with differential life-history traits and adaptation to diverse ecological environments (Muscedere & Traniello, 2012; Gordon *et al.*, 2019; Arganda *et al.*, 2020; Li *et al.*, 2022; Muratore *et al.*, 2022).

Despite the valuable insights obtained from prior research, these studies have primarily focused on describing the correlative relationship between volumetric, neurochemical or transcriptomic features of the entire brain and the behavioral tendencies of distinct ant castes. To gain a deeper understanding of the neural basis underlying the division of labor in ants, it is crucial to advance to finer organizational levels, moving beyond the analysis of whole-brain features. This includes examining how ant brains function at the molecular, cellular, circuit, and organ levels. The pursuit of this research aim could start by characterizing the caste-specific neural features, such as cellular number, soma distribution, projection pattern, and gene expression, with molecularly labeled and functionally important neural subpopulations.

Dopamine is a crucial neuroactive molecule which plays a central role in regulating numerous aspects of animal physiology and behavior in both vertebrates and invertebrates. Dopamine acts as an important catecholamine neurotransmitter in the central nervous system. It is synthesized in dopamine neurons and released into the synaptic cleft, acting by specifically activating dopamine receptors located on the postsynaptic membrane (Mustard *et al.*, 2005). The biosynthesis of dopamine is a multistep process that begins with the amino acid tyrosine and involves several enzymatic reactions. Tyrosine is first hydroxylated by tyrosine hydroxylase (TH, also known as ple), a key rate-limiting enzyme in dopamine synthesis, to produce L-3,4-dihydroxyphenylalanine (L-DOPA). L-DOPA is then decarboxylated to produce dopamine under the action of DOPA decarboxylase (DDC) (Blenau & Baumann, 2001; Beaulieu & Gainetdinov, 2011). After dopamine is synthesized, the vesicular monoamine transporter (VMAT) transports it from the cytoplasm into the synaptic vesicles, where it is stored and ready for release (Yaffe *et al.*, 2018).

In the fruit fly, approximately 282 dopamine neurons in the central brain regulate a wide range of behaviors (Nässel & Elekes, 1992; Mao & Davis, 2009) including motor activity, arousal, learning and memory, circadian rhythm, sleep, aggression, and courtship (Yamamoto & Seto, 2014). In ants, dopamine is involved in regulating reproduction, foraging, aggression, and nestmate interactions (Barbero *et al.*, 2023). For example, in *Solenopsis invicta* high dopamine levels are associated with reproduction and dealation of virgin females following queen separation (Boulay *et al.*, 2001). Meanwhile, high dopamine levels promote workers' labor transition from nurses to foragers by N^6-methyladenosine modification of dopamine receptor 1 and dopamine transporter (Chen *et al.*, 2024). In *Diacamma*, dopamine lev-

els in the brains of reproductive workers were significantly higher compared to age-matched nonreproductive workers. Under dopamine induction, workers exhibited oocyte growth, but no increase in aggression, indicating dopamine has gonadotropic effects (Okada *et al.*, 2015). In *Myrmica scabrinodis*, dopamine levels in the brain were inversely correlated with aggressive behavior in worker ants (Mannino *et al.*, 2018). In *Pheidole*, the dopamine titer of the brain in major workers was significantly higher than minor workers (Giraldo *et al.*, 2013). In *Formica japonica*, starved or undernourished workers exhibit low dopamine levels, which can be restored through trophallaxis (Wada-Katsumata *et al.*, 2011). In red harvester ants, dopamine plays a crucial role in regulating collective foraging activity in response to changes in humidity (Friedman *et al.*, 2018). In *Lasius niger*, appetitive olfactory learning depends on both octopamine and dopamine signaling (Wissink & Nehring, 2021) and these aminergic signals as well affect foraging and orientation behavior guided by geomagnetic fields (Mannino *et al.*, 2023). Although the dopamine system is clearly pivotal in regulating caste-specific behaviors in ants, previous studies primarily focused on the correlative relationship between dopamine levels and behavioral tendencies. The anatomical features and distributions of dopamine neurons in ant brains remain largely unexplored. Furthermore, how the dopaminergic system is developmentally and functionally differentiated across ant castes is yet to be systematically investigated.

In this study, we generated a specific antibody for TH of pharaoh ants. Using this tool, we systematically compared the cell number and spatial distribution of dopamine neurons across all 4 castes (worker, gyne, queen, and male) and identified caste-specific anatomical features of these neurons. Through the single-cell transcriptomics from pharaoh ant whole brains, we uncovered distinct molecularly defined dopamine clusters and validated the expression of multiple neuropeptide genes within specific dopamine clusters. Notably, we identified a subset of dopamine neurons that may regulate mating behaviors and are exclusively present in males and gynes. This study provides a foundation for future research to pin down the function of specific dopamine neuronal subsets in governing reproductive division of labor across ant castes.

Materials and methods

Biological samples

We chose *Monomorium pharaonis* as our study organism due to its simple and well-defined social structures and distinct division of labor. Meanwhile, this species offers several practical advantages, including ease of maintenance, a short developmental period (about 45 d), frequent production of reproductive castes and the ability to maintain large colonies, all of which facilitate experimental research. A typical *M. pharaonis* colony consists of 4 distinct castes, worker, gyne, queen, and male (strictly speaking, gynes and queens represent different life stages of the same reproductive caste, whereas males are not typically classified as an independent caste. However, in this study, we use the term "caste" in a broader sense for maximizing convenience of expression.). Worker, gyne, and queen are all females that develop from fertilized diploid eggs. Workers entirely lost their reproductive capabilities, performing all the daily tasks supporting the colony, including nursing, brood-caring, and foraging. Gynes are reproductive females who temporarily remain with the colony, once successfully mated would become a true queen and never remate in their lifetime. Queens, on the other hand, are inseminated reproductive females solely responsible for egg-laying, and they exhibit remarkably extended lifespans. In contrast, males develop from unfertilized haploid eggs and exist solely to inseminate gynes, typically dying soon after mating (Baer, 2011).

The original colony of *M. pharaonis* was collected in 2016 from a resident house in Mengla, Xishuangbanna, Yunnan Province, China, and split into 100s of subcolonies in the laboratory in the subsequent years. All colonies were reared at 27 °C, 65% relative humidity and a 12/12 h light/dark cycle. New gynes and males were induced in newly split colonies where inseminated and egg-laying queens were removed, and male pupae were collected into a separate rearing box to prevent the newly hatched gynes becoming inseminated. The queens were collected using the following procedure. Newly eclosed gynes were collected and placed into a new rearing box containing workers and brood. After waiting for 3 d (3rd d posteclosion), males were introduced into the rearing box to allow mating for 2 d. The males were removed on the 5th d, by which time some gynes had successfully mated and transitioned into queens. These potentially inseminated "queens" were then reared for an additional 3–6 months until they reached an age when they were actively engaged in egg-laying. Prior to dissecting their brains for staining, we confirmed their insemination status by examining their spermathecae to ensure they were indeed inseminated. Workers were randomly collected out of the nests. For hybridization chain reaction (HCR) and immuno-histo-chemistry (IHC) experiments, 7–10 d old gynes, 3–6 months old queens were used; the ages of males and workers were not recorded.

Brain dissection

Ants were anesthetized on ice, and then heads were dissected in ice-cold phosphate-buffered saline (PBS: 0.1% diethyl pyrocarbonate [DEPC] treated) under a stereomicroscope (Nikon, SMZ745). The forceps (Dumont 0209-5-PO 5#) were inserted gently into the mouthparts and the head shell of the ant was attentively torn apart. After carefully removing the muscles and other surrounding tissue, the brain was extracted. We carefully removed the attached trachea and ocelli (absent in workers). The brains were collected in Eppendorf tubes for fixation with 4% PFA (paraformaldehyde, 0.1% DEPC treated) at room temperature for 20 min.

IHC staining of dopamine neurons in the brains

We performed costaining using an anti-TH antibody to label dopamine neurons and the nc82 antibody to visualize the brain's neuropil structure. nc82 is a monoclonal antibody recognizing *Drosophila* Bruchpilot protein, ubiquitously labeling presynaptic active zones. It is widely used to label neuropils in *Drosophila* and other insects, demonstrating distinct brain compartments. Fixed brains were rinsed with PBSTw (0.1% Tween-20 dissolved in PBS) for 5 min, 3 times. The brains were then treated with 5% PBSTx (5% Triton X-100 dissolved in PBS) for 8 min, followed by 3 PBSTw rinses for 5 min. The brains were blocked with 1 mL PAT (1% bovine serum albumin in 1% PBSTx) for 30 min at room temperature, followed by primary antibody (anti-TH antibody 1 : 1 000 dissolved in PAT, nc82 antibody 1 : 250 dissolved in PAT) incubation overnight at 4 °C. The brains were rinsed with 1 mL 1% PBSTx for 5 min, 3 times, then incubated with secondary antibody (1 : 1 000 dissolved in PAT) for 2 h at room temperature. Brains were rinsed with PBSTw for 5 min, 3 times. Anti-TH antibody was customized antibody produced by ABclonal Technology Co., recognizing 140–340 amino acids of tyrosine 3-monooxygenase isoform X1 (Sequence ID: XP_012540345.1) in *M. pharaonis*. Alexa Fluor 488 (Thermo Fisher, A30052) was used for the detection of nc82 and Alexa Fluor 633 (Thermo Fisher, A-21052) was used for TH. The stained brains were imaged with a confocal laser scanning microscope (Nikon, A1).

HCR RNA-FISH (fluorescence in situ hybridization) of target transcripts in the brains

We generally followed the HCR RNA-FISH protocol provided by Molecular Instruments (www.molecularinstruments.com) for whole-mount fruit fly embryos in the HCR experiments, but with modifications for preparation steps of fixed whole-mount ant brains. Fixed brains were rinsed with PBSTw for 5 min. The brains were rinsed with ice-cold methanol for 5 min, then with 3 : 1, 1 : 1, 1 : 3 methanol : PBSTw for 5 min each, followed by 2 PBSTw rinses for 5 min. The brains were treated with 5 μg/mL proteinase K for 5 min, followed by 3 PBSTw rinses for 5 min. After that, the brains were fixed with 4% PFA (0.1% DEPC treated) for 20 min at room temperature, followed by 5 PBSTw rinses for 5 min. Thereafter, the detection and amplification steps were performed following the referenced protocol. The *Nlg2* messenger RNA (mRNA) (XM_012685917), *TH* mRNA (XM_012684891.3), and *Ms* mRNA (XM_012680598.3) HCR probe sets (Table S2) syntheses were performed by Sangon Biotech (Shanghai, China). And amplifiers and buffers were commercially purchased from Molecular Instruments, Inc. We used Alexa Fluor 488 for the detection of *Nlg2*, Alexa Fluor 594 for *TH* mRNA. The stained brains were imaged with a confocal laser scanning microscope (Nikon, A1).

Small nuclear RNA sequencing (snRNA-seq) reclustering and analysis

For snRNA-seq analyses, we used DNBelab C Series Single-Cell Library Prep Set (MGI Tech Co.) reads from a previous study that reports the single-cell transcriptomics of pharaoh ant whole brains (Li *et al.*, 2022). We used STARsole to realign the original sequencing data and regenerate each library's Unique Molecular Identifier (UMI) matrix removing the background noise by CellBender (Fleming *et al.*, 2019). These steps are necessary as they improve data utilization, resulting in a significant increase in the number of available cells and transcripts per cell in each library. Then we integrated the library using the latest Harmony method, using the Leiden algorithm for clustering, and ultimately obtained 6 479 dopaminergic neurons (DANs) cell populations specifically expressing Vmat and DAT. Finally, based on this cluster of cells, we conducted a reclustering for DANs. Marker genes for each cluster were identified by the FindAllMarkers function with the Wilcoxon Rank Sum test (min.pct = 0.25, logfc.threshold = 0.25, test.use = "wilcox," only.pos = TRUE). We presented the marker gene list information of *M. pharaonis* DANs by referring to the display method of the marker gene list for single-cell reclustering of *D. melanogaster* DANs (Ma *et al.*, 2023).

Gene Ontology (GO) annotations and enrichment analyses

The protein-coding genes of the *M. pharaonis* were reported in a previous study (Gao *et al.*, 2020). GO of the *M. pharaonis* protein-coding genes was assigned according to the GO annotation of their orthologs in *D. melanogaster*. One-to-one orthologs between *M. pharaonis* and *D. melanogaster* were built as mentioned above. The *M. pharaonis* genes that could not be annotated by the orthologous method were further aligned to the UniProt database (release-2020_04) using BLASTP with parameters (-F F -e 1×10^{-5}). The best hit of each query gene was then retained, on the basis of its BLASTP bit score, and the GO annotations of that best hit were assigned to the query gene. The combination of these 2 methods allowed us to assign GO annotation to 76% of the *M. pharaonis* protein-coding genes, which is considerably higher than the 56% previously reported (Gao *et al.*, 2020). Fisher's exact tests were used to examine whether the upregulated differentially expressed genes (DEGs) in a focal cell cluster (or a group of clusters) were significantly enriched in a specific GO term in relation to the background genes. This procedure compared the number of upregulated DEGs annotated to this GO term, the number of upregulated DEGs not annotated to this GO term, the number of background genes annotated to this GO term and the number of background genes not annotated to this GO term. The background genes were defined as all genes except for the upregulated DEGs with mean expression level (CP10K) > 1 across the cell clusters of interest. *P*-values were adjusted by false discovery rate (FDR) following the Benjamini–Hochberg procedure77, and GO terms with FDR < 0.05 and gene number ≥ 2 were considered to be significantly enriched.

Apoptosis detection of the dopamine neurons with Cleaved Caspase-3 antibody in the brains

We detected apoptotic dopamine neurons in the queen brain (7 d after mating) by staining Cleaved Caspase-3 and *TH*. The brains were stained by HCR with *TH* probes then rinsed by PBSTw for 5 min and repeated 3 times. After that, the brains were blocked by PAT for 30 min. The brains were incubated with the Cleaved Caspase-3 (Asp175) antibody (CST, 9661T), antibody 1 : 1 000 dissolved in PAT and incubated overnight at 4 °C. The brains were rinsed then incubated with secondary antibody (Alexa Fluor 488, 1 : 1 000 dissolved in PAT) for 2 h at room temperature. The rinsed and stained brains were imaged with a confocal laser scanning microscope (Nikon, A1).

Data collection and analysis

The stained brains were imaged from both anterior and posterior views. Whole brains were scanned as series of sections at intervals of 5 μm using a 20×/0.75 objective with adjusted digital zoom. For anterior view, we obtained 7 brain images for workers, 3 for gynes, 13 for queens, and 4 for males. For posterior view, we obtained 6 brain images for workers, 3 for gynes, 11 for queens and 5 for males. Since not all dopamine clusters within the same brain were uniformly well-stained, we selected high-quality images from different brains for each cluster to ensure reliable counting of dopamine cell numbers within that specific cluster. Ultimately, more than 3 biological replicates were used to count the cell body numbers of every cluster of DANs in each brain hemisphere. These images were captured by confocal laser scanning microscope (Nikon, A1) and then processed using ImageJ software (version 4.8.2). All images were taken at a resolution of 1024×1024 pixels and were saved as ND2 files. The numbers of cell bodies were manually counted (less than 10) or by Imaris (Oxford Instruments) software (more than 10). Statistical analyses were performed using GraphPad Prism software and all data were evaluated via one-way analysis of variance (ANOVA) followed by a Newman–Keuls multiple comparison test.

Results

The distribution of dopamine neurons in the brains of M. pharaonis

To address whether and how the dopamine system is involved in regulating complex social behaviors across ant castes, we first need a clear and accurate way to map the distribution of dopamine neurons in the ant brain. We generated a customized poly-clonal antibody targeting *M. pharaonis* TH. To verify the specificity of the antibody, we performed a double-labeling experiment of *TH* mRNA with specific HCR probes and TH protein with the customized antibody. We found that the neuronal soma detected by IHC staining (Fig. 1A, B) entirely overlaps with those detected by HCR staining (Fig. 1C, D), indicating that the antibody specifically labels the *TH*-expressing dopamine neurons (Fig. 1E, F). We examined the brain from both anterior and posterior sides, we could see that the IHC staining captures all dopamine neuron clusters; in addition, the effect of IHC staining is better

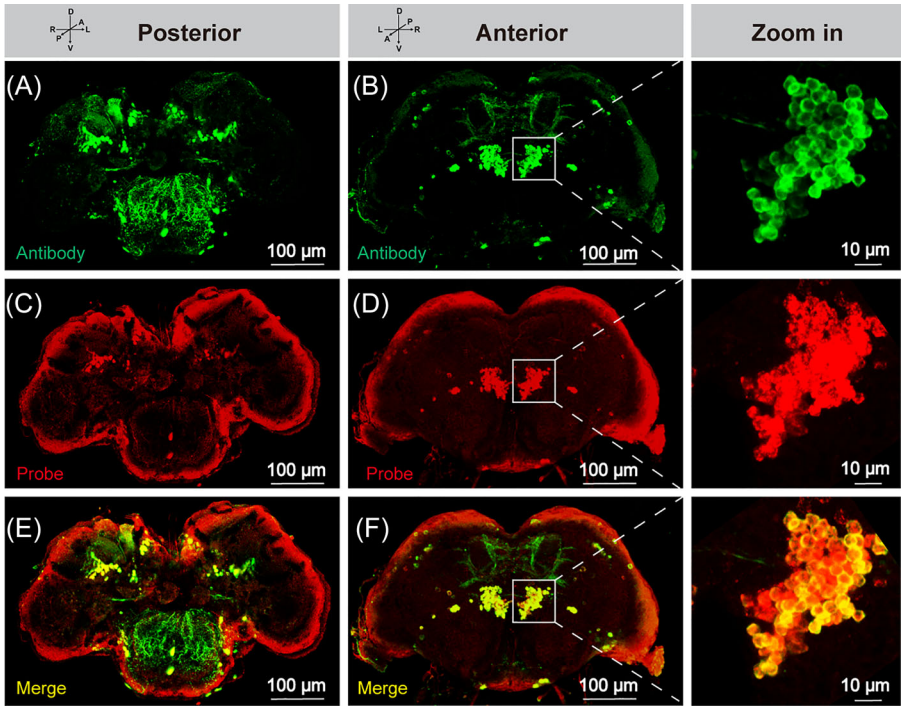

Fig. 1 The specificity of *Monomorium pharaonis* anti-TH antibody. Anterior and posterior views of IHC staining with antibody (A, B) and HCR staining with probe in the brain of pharaoh ant (C, D). (E, F) Merged image of IHC and HCR staining. Zoom-in of the boxed region in (B), (D), and (F). Red indicates *TH* transcript detected by HCR method; green indicates TH protein detected by IHC method; yellow indicates merged signal. The brain orientation is indicated: A = anterior, P = posterior, D = dorsal, V = ventral L = left, R = right. HCR, hybridization chain reaction; IHC, immuno-histo-chemistry; TH, tyrosine hydroxylase.

than HCR staining, the signals are concentrated in the cytoplasm and the projections of the neurons are also detected (Fig. 1). Therefore, in the following experiments, we chose the IHC method to systematically characterize dopamine systems across 4 castes of pharaoh ant.

We collected plentiful samples of the 4 castes from pharaoh ant colonies and performed IHC staining. We annotated the dopamine neuronal clusters of pharaoh ants according to their spatial distributions by referring to that of fruit flies (Nässel & Elekes, 1992; Mao & Davis, 2009; Xie *et al.*, 2018). We identified a total of 17 clusters of dopamine neurons that are distinctively distributed in pharaoh ant brains (Fig. 2C–J). Clusters of PAL, PAM1, PAM2, PAL2, D1, and DAM can be observed from the anterior side (Fig. 2A), clusters of PPM1, PPM2, PPM3, PPL1, PPL2, PPL3, DPL, SP1, SVP, VUM1, and VUM2 can be observed from the posterior side (Fig. 2B). These cluster names are acronyms indicating the spatial localizations of the cell bodies, and their corresponding full names are detailed in Table S1. The total number of dopamine neurons is different across the 4 castes: workers have around 322 dopamine neurons, gynes 374, queens 343 and males 431 (Table S1). Although the cell number of each cluster varies, all the 17 clusters are present across the 4 castes (Table S1).

To address whether social living is correlated with specific neural circuit remodeling, especially how the dopamine system is differentiated between solitary and social insects, we performed a neuroanatomical comparison on the cluster distribution and cell number of the dopamine system between flies and ants. Since the brains of *M. pharaonis* male and worker are extremely specialized for different social roles, while the brain of the gyne is generally totipotent, representing the ancestral state of social insect (Li *et al.*, 2022), we therefore chose *M. pharonis* gyne and *D. melanogaster* female to do the comparison. In the brain of *M. pharonis* gyne, ~374 dopamine neurons are detected by anti-TH antibody and in the brain of *D. melanogaster* female, ~282 dopamine neurons are detected by anti-TH antibody (Mao & Davis, 2009). The major dopamine neuron clusters in the central brain of pharaoh ants are located at regions comparable to that of fruit flies. Specifically, these clusters are found in: PAM1, PAM2 and PAL, PAL2 located in the anterior side; PPM1/2, PPM3, PPL1/3, and PPL2 located in the posterior side (Fig. 2A–N). Other dopamine neuron clus-

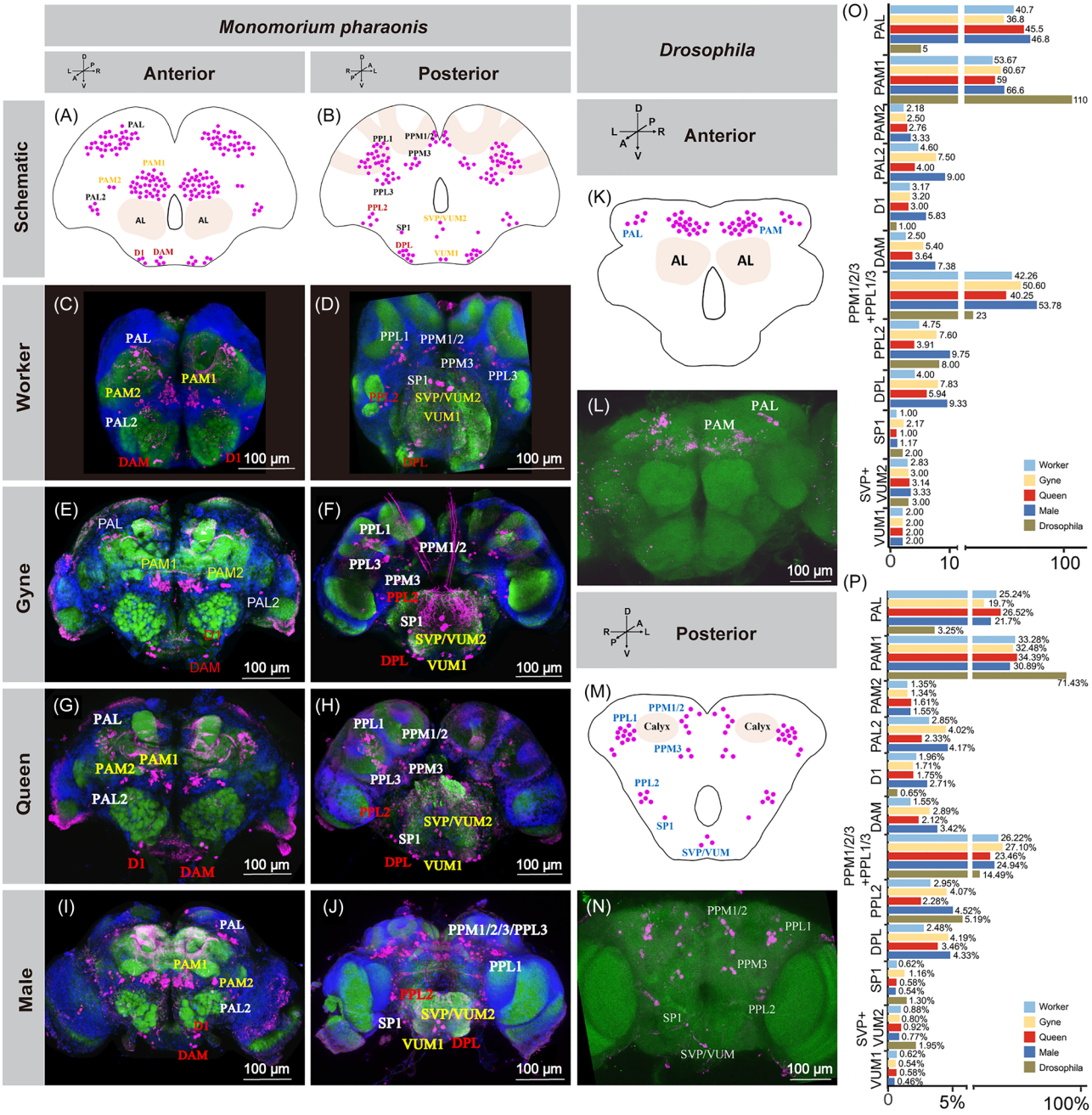

Fig. 2 The brain dopaminergic system of *Monomorium pharaonis* ant. Anterior and posterior views of the brain show different dopamine clusters. (A, B) Schematic representation of distribution of dopamine neurons in the brain of adult pharaoh ant gyne. (Small magenta dots indicate dopamine neuron cell body; red font-labeled clusters having different cell numbers across castes, yellow font-labeled clusters having uniform cell numbers across castes and black font-labeled clusters where accurate cell numbers are not determined). (C–J) The distribution of dopamine neurons across castes in the brains of *M. pharaonis* viewed from both anterior and posterior sides. Blue indicates 4′,6-diamidino-2-phenylindole, green indicates nc82, magenta indicates dopamine neuron cell body detected by IHC. The red font indicates clusters having different cell numbers across castes, yellow font indicates clusters having uniform cell numbers across castes and white font indicates clusters in which accurate cell numbers are not determined. (K–N) Distribution of dopamine neurons in the female brain of adult *Drosophila*. In the schematic representation, small magenta dots indicate dopamine neuron cell bodies (K, M). In the staining image, green indicates nc82, magenta indicates dopamine neuron cell body detected by HCR method (L, N). The brain orientation is indicated: A = anterior, P = posterior, D = dorsal, V = ventral L = left, R = right. (O) The

ters are mainly located at the brain periphery, and their counterpart neurons in the flies are variably labeled. Several clusters in ants contain remarkably more cells than in flies, such as PAL and PPL1/3. There are around 12 cells in PPL1+PPL3 clusters per brain hemisphere in flies (Nässel & Elekes, 1992; Mao & Davis, 2009) while a much higher number of cells (ca. 39 in gyne) can be detected in these clusters per brain hemisphere in ants (Fig. 2O and Table S1).

Single-cell transcriptomics atlas of dopamine neurons in M. pharaonis *brains*

A previous single-cell transcriptomics atlas of pharaoh ant whole brains has identified clusters of monoaminergic neurons that preferentially express Vmat (Li *et al.*, 2022). *Vmat* encodes a protein responsible for packaging the monoamine neurotransmitters into secretory vesicles (Greer *et al.*, 2005), therefore the *Vmat*+ monoaminergic clusters supposedly combine dopamine, serotonin, and octopamine neurons. By reanalyzing the single-cell transcriptomics datasets, we identified 6 479 monoaminergic neurons and divided these neurons into 14 distinct transcriptional subclusters (Fig. 3A and Table S3), including 1 serotonin subcluster (c8, preferentially expressing *Trh*), 2 octopamine subclusters (c10 and c14, preferentially expressing *Tdc2* and *Tbh*) and 11 dopamine subclusters (preferentially expressing *ple* and *DAT*).

We identified a repertoire of marker genes that are preferentially expressed in unique subclusters (Table S3), including neuropeptides (e.g. *Ms*, *SIFa*, *Dh31*, *Allatostatin-C*), cell surface molecules (e.g. *Nlg*, *Nrx*, *DIP*, *Dpr*), receptors for neurotransmitter/neuropeptide (e.g. *Oamb*, *AstA-R1*, *Dh44-R1*, *GABA-B-R3*) (Fig. S1), hormone signaling related molecules (e.g. *gce*, *EcR*, *Hr3*) and transcriptional regulators (e.g. *Fer2*, *mirr*, *erm*, *dati*) (Fig. 3C). *VGlut* (vesicular glutamate transporter) is specifically expressed in c7, *Gad1* as well as *ChAT* are expressed in c1, and *ChAT* is specifically expressed in c5, suggesting that the dopamine neurons coemploy glutamate, γ-aminobutyric acid or acetylcholine as their fast neurotransmitters. We performed GO analysis of the enriched marker genes in dopamine subclusters (Table S4). Interestingly, we found subcluster c2 is enriched in the GO term "positive regulation of cell death" and c3 is enriched in "cell population proliferation," suggesting that these dopamine neurons may undergo apoptosis or neurogenesis during adulthood and may be responsible for regulating adult behavioral plasticity, while c8 and c12 are enriched in GO terms of chemical sensation, indicating that these neurons may be involved in olfactory and gustatory communications.

To validate the marker gene expression in specific dopamine subclusters, we conducted a series of colabeling experiments with *TH* probe and probes for several neuropeptide marker genes. Neuropeptide genes *Ms* (*myosuppressin*) and *AstC (Allatostatin-C)* were identified to be markers for subcluster c9 (Fig. S1). We validated that these 2 neuropeptide genes are indeed specifically coexpressed in a subset of PPL3 dopamine neurons (Fig. 3B). Other neuropeptide marker genes are also validated to be expressed in specific dopamine neurons, for example, *CAPA* (*capability*) is expressed in a subset of DPL; *Dh31* (*diuretic hormones*) in subsets of PAL, PPL1 and PPL3; *TK* (*tachykinin*) in a subset of PPL3 and *Nplp1* (*neuropeptide-like precursor 1*) in subsets of PAL, PAL2, PAM, and PPL1-3 (Fig. S2). These results confirmed the accuracy of our subclustering analysis, while at the same time, indicated that the transcriptional clusters may not precisely recapitulate the anatomical ones, as is evidenced that the markers for unique transcriptional clusters can express in different anatomical clusters, and the same anatomical clusters can be labeled by markers for different transcriptional clusters. Characterizing the transcriptional signatures of dopamine neuron subsets in pharaoh ants offers a valuable resource for further dissecting their diverse functional roles. It can also enhance our understanding of how dopamine neurons differentiate to regulate specialized behaviors associated with distinct social roles in ants.

Comparison of dopamine system across castes in M. pharaonis

By comparing the distribution and cell number of the above identified dopamine clusters across the 4 *M. pharaonis* castes, we found that 5 clusters had uniform cell numbers across 4 castes (Fig. S3I–L), including PAM1/2, SVP, VUM1/2 (one-way ANOVA: PAM1: $P = 0.3118$, PAM2: $P = 0.0385$, SVP/VUM2: $P = 0.5912$, VUM1: *P*- and *F*-values not available since the numbers of VUM1 neurons keep consistent within and between groups). The first 2 clusters can be detected in the anterior side and were located above the antennal lobe (Fig.

comparison of dopamine neuron cell numbers of different clusters across 4 castes of *M. pharaonis* and *Drosophila*. (P) The comparison of dopamine neuron relative abundance of different clusters across castes of *M. pharaonis* and *Drosophila*. HCR, hybridization chain reaction; IHC, immuno-histo-chemistry.

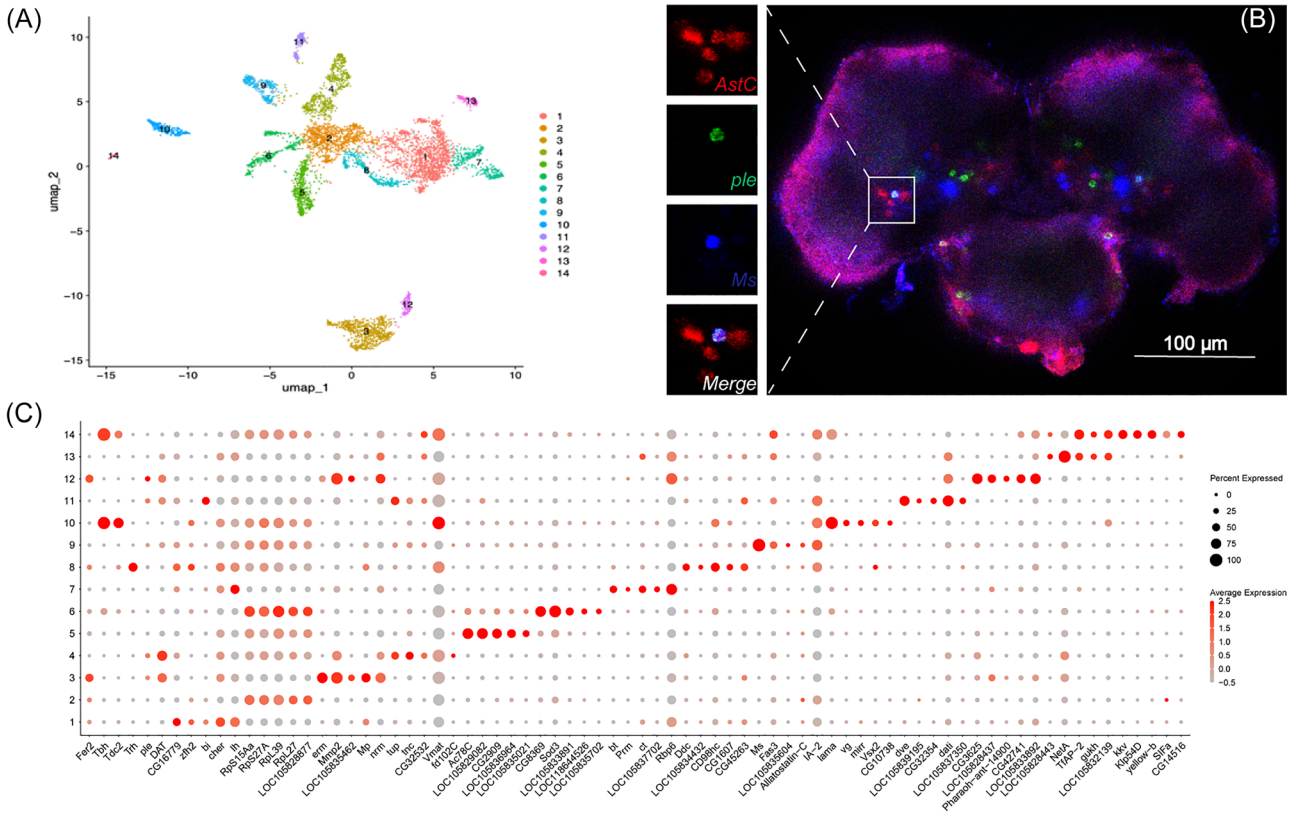

Fig. 3 Single-cell transcriptomics atlas of dopamine neurons in *Monomorium pharaonis* brain. (A) Uniform Manifold Approximation and Projection plot showing monoaminergic neuron subclusters in *M. pharaonis* brain. (B) Costaining of *AstC* (red), *ple* (green) and *Ms* (blue) by HCR in a subset of PPL3 neurons. Zoom-in of the left white dotted box of B. (C) Dot plot showing the expression of marker genes in respective cell clusters. Dot color indicates average expression of a gene and dot size indicates percentage of cells within each cluster expressing the particular marker gene. HCR, hybridization chain reaction.

S3A–D) while the other 3 can be detected in the posterior side and were located in the subesophageal zone (SEZ) (Fig. S3E–H and Table S1).The cell numbers and spatial distributions of SVP and VUM1/2, were similar not only across the 4 ant castes but also in the fly (Nässel & Elekes, 1992), indicating that these dopamine neurons may play conserved functions for fundamental life activities.

There are 4 clusters that are significantly differentiated across ant castes, including DAM, D1 (one-way ANOVA: DAM: $P < 0.0001$, D1: $P < 0.0001$), in the anterior side (Fig. 4A–D) and DPL and PPL2 (one-way ANOVA: DPL: $P < 0.0001$, PPL2: $P < 0.0001$; ANOVA was followed by Newman–Keuls multiple comparison test) in the posterior side (Fig. 4E–L). The cell numbers of all these clusters were highest in males among the 4 castes; the cell numbers of DAM, DPL, and PPL2 were higher in gynes compared to workers; and cell numbers of DPL and PPL2 were decreased in queens compared to gynes (Fig. 4M–P). The results indicate that subsets of dopamine neurons are differentiated by sex, caste, and reproductive role in an ant colony, rewiring the neural circuit for distinct social roles within an ant colony.

Additionally, 8 clusters—PAL, PAL2, PPM1/2, PPM3, PPL1, PPL3, and SP1—remain undetermined in terms of their differentiation across castes, due to the following challenges: (1) the abundant cell numbers and densely packed cell bodies of PAL, PPM1/2/3, PPL1, and PPL3 hindered accurate counting; (2) PPM1/2/3, PPL1, and PPL3 are clustered together in males, preventing clear separation of individual clusters; and (3) PAL2 and SP1 exhibited remarkable variations across biological replicates within the same caste. Given these limitations, we refrained from drawing conclusions about their caste-specific differentiation.

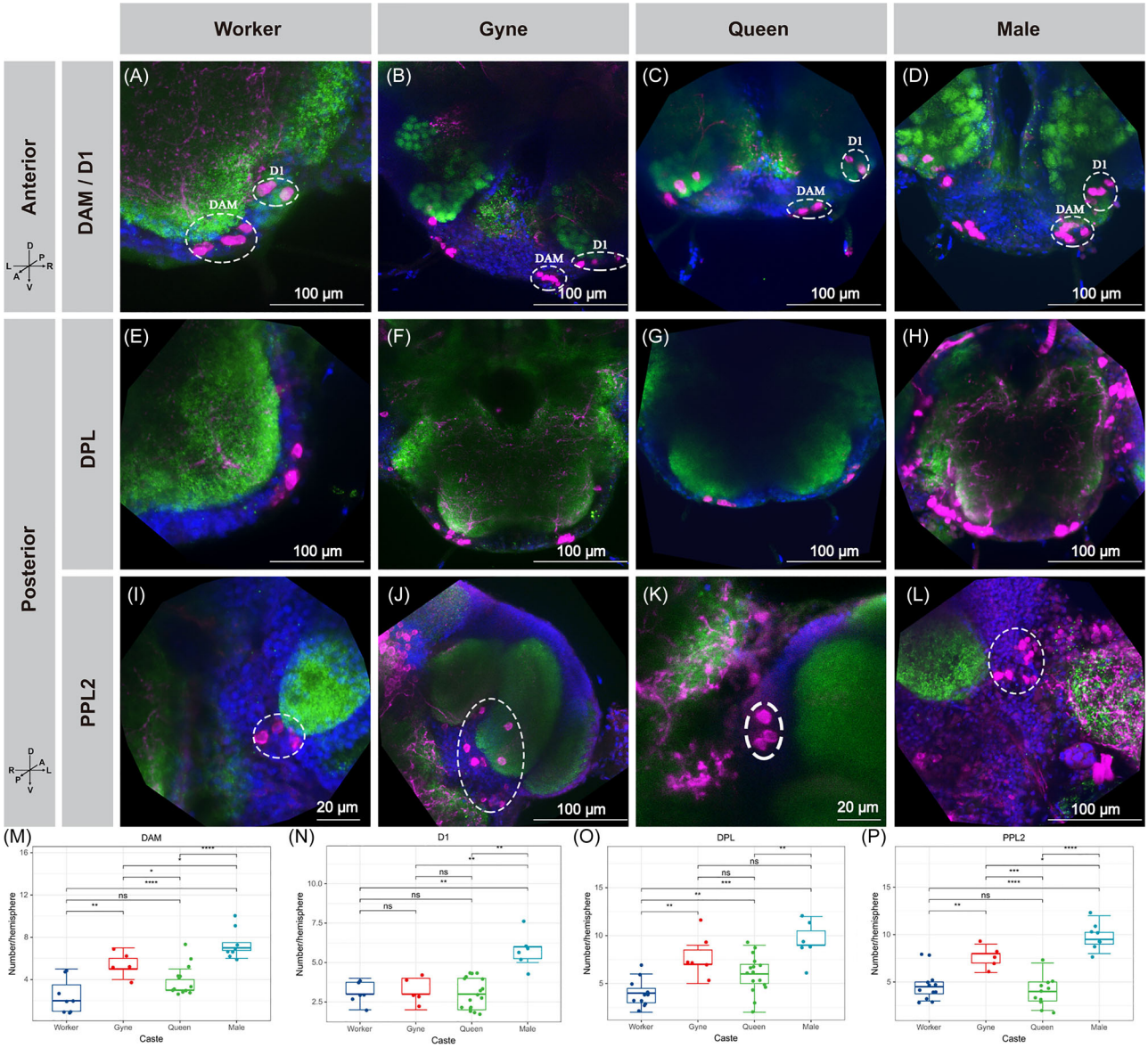

Fig. 4 Differentiated dopamine neurons across castes. (A–D) DAM and D1 clusters of 4 castes viewed from the anterior side. (E–H) DPL cluster of 4 castes viewed from the posterior side. (I–L) PPL2 cluster of 4 castes viewed from the posterior side. (M–P) Box plot showing the cell number per hemisphere of the differentiated dopamine clusters (one-way analysis of variance followed by Newman–Keuls multiple comparison test. Asterisk represents $P < 0.05$). Blue in A–L indicates 4′,6-diamidino-2-phenylindole; green indicates nc82; magenta indicates dopamine neuron cell body detected by IHC. The brain orientation is indicated: A = anterior, P = posterior, D = dorsal, V = ventral L = left, R = right. IHC, immuno-histo-chemistry.

PPL2b neurons potentially involved in reproductive division of labor

Among the caste differentiated dopamine cell clusters, PPL2 is of particular interest. The PPL2 cluster in fruit fly is crucial for mating behavior (Kuo *et al.*, 2015; Chen *et al.*, 2017). Elevating dopamine levels in these neurons could suppress the decline of mating drive in aged male flies (Kuo *et al.*, 2015) and activating these neurons could induce higher sexual drive in the male flies to court other males (Chen *et al.*, 2017). We found that ant PPL2 neurons consist of 2 subsets: PPL2a, characterized by slightly smaller cell bodies, and PPL2b, with larger cell bodies, were found exclusively in gynes and males,

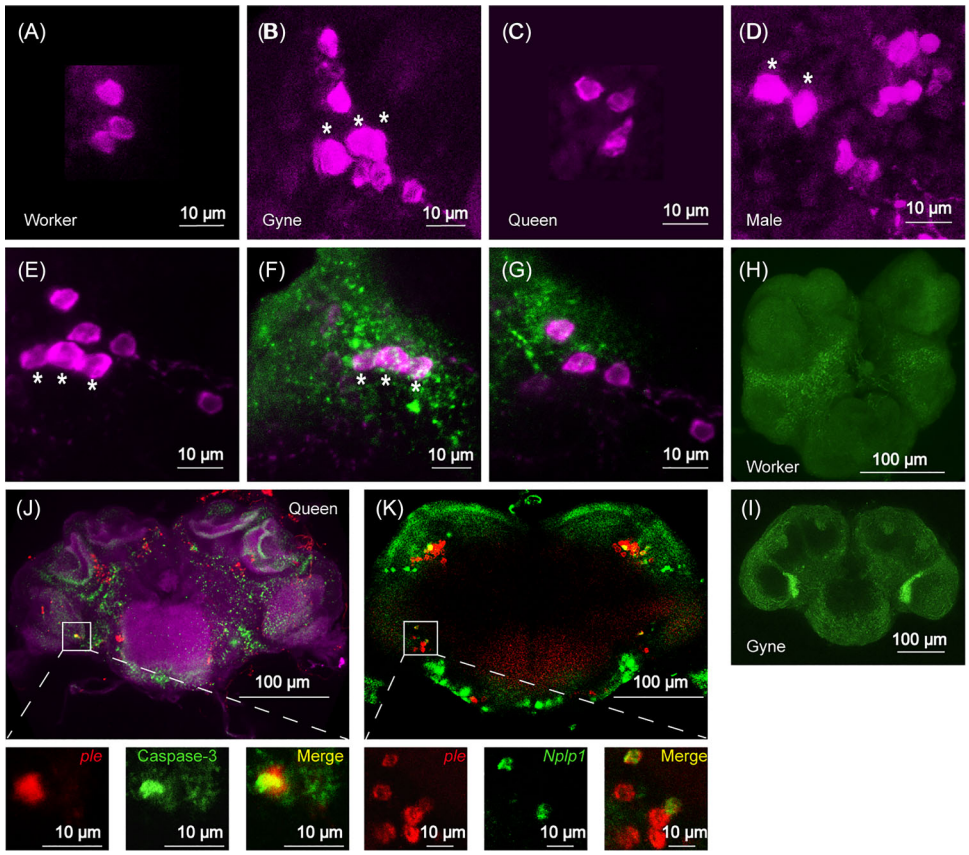

Fig. 5 PPL2b neurons differentiated across castes. (A–D) PPL2 cluster across 4 castes. PPL2 can be subdivided into smaller PPL2a and larger PPL2b. PPL2b is only found in gynes and males, labeled with asterisks. (E–G) Costaining of *Nlg2* gene and PPL2 neurons in gyne brain indicates differential spatial locations of PPL2a and PPL2b. The entire PPL2 cluster is shown, PPL2b is labeled with asterisks (E), the cell bodies of PPL2b neurons are immediately approximate to *Nlg2*-expressing region (F) but not PPL2a (G). (H, I) *Nlg2* is only detected in the gyne brain while it is absent in the worker brain. Magenta in A–G indicates dopamine neuron cell body detected by IHC; green indicates *Nlg2* signals detected by HCR. (J) Costaining of *ple* by HCR (red) and Cleaved Caspase-3 by IHC (green) in PPL2 neurons, magenta indicates nc82. (K) Costaining of *ple* (red) and *Nplp1* (green) in PPL2 by HCR. HCR, hybridization chain reaction; IHC, immuno-histo-chemistry.

while being absent in workers and queens (Fig. 5A-D). In fruit flies as well as blow flies, PPL2 cluster is also divided into 2 different subsets, PPL2a and PPL2b, which are distinguished by different cell body sizes and projection patterns (Nässel & Elekes, 1992; Mao & Davis, 2009). PPL2b in blow flies contain larger neurons and extend projections to lobula and lobular plate while PPL2a are located more dorsal and do not innervate the lobula complex (Nässel & Elekes, 1992). In ants, we found that the spatial localizations of PPL2a and PPL2b in gyne brains are also differentiated, whereby the cell bodies of PPL2b neurons are immediately approximate to *Nlg2*-expressing lobular regions (Fig. 5E, F), whereas the cell bodies of PPL2a neurons are distant away from these regions (Fig. 5E, G). In pharaoh ants, *Nlg2*+ neurons preferentially express genes associated with courtship regulation (Li *et al.*, 2022). Additionally, the *Nlg2*-expressing lobular region is prominently present in gyne, queen and male while it is totally absent in workers (Li *et al.*, 2022) (Fig. 5H, I). The fly counterparts (T4/T5 neurons) of *Nlg2*+ neurons are involved in locomotion detection and visual target-induced courtship behavior (Schnell *et al.*, 2012; Ribeiro *et al.*, 2018). At the same time, we found that *Nplp1* (a marker gene identified by reclustering analysis of dopamine neurons from whole-brain single-cell transcriptomics atlas) expressed in part of PPL2 neurons, further confirming the heterogeneity of these neurons (Fig. 5K). To address whether PPL2b neurons are lost by apoptosis in mature queens, we performed IHC staining to detect apoptotic signals with Cleaved Caspase-3 anti-

body in the queen brain (7 d after mating). We found that PPL2 neurons were positive for Cleaved Caspase-3 signals, suggesting the PPL2b neurons in the queen brain undergo apoptosis soon after successful mating (Fig. 5J).

Discussion

In this study, we have systematically characterized the anatomical features of the central brain dopamine system across all 4 adult castes of pharaoh ants, and identified differentiated dopamine neurons that potentially play a crucial role in regulating mating behavior. We also observed an expansion of certain dopamine neurons in ants compared to their counterparts in flies, suggesting these neurons may contribute to the rewiring of the mushroom body circuit, potentially supporting advanced cognitive capabilities in social insects. We also identified a repertoire of transcriptomic markers to further subdivide the heterogeneous dopamine neurons, which may provide an entry point for further delineating the neural mechanisms underlying division of labor in ants.

Subset of dopamine neurons critical for social living

Dopamine likely plays a critical role in modulating social interactions, largely owing to its vital function in regulating learning and memory processes. We found there are ∼322 to ∼431 dopamine cells in pharaoh ant and there are ∼400 to ∼450 in the honey bee brain hemisphere (Tedjakumala *et al.*, 2017), while there are ∼300 in files (Nässel & Elekes, 1992; Mao & Davis, 2009). Further, we found the cell numbers of several clusters of dopamine neurons are notably expanded in ants compared to flies, with the PPL1/3 being of particular interest. In flies, PPL1 neurons project to the vertical lobes, junction area, heel, and distal peduncle of mushroom bodies, with subsets innervating distinct zones of mushroom body lobes (Mao & Davis, 2009). These neurons play a critical role in regulating learning and memory in flies (Adel & Griffith, 2021), encoding aversive reinforcement signals in the mushroom body (Claridge-Chang *et al.*, 2009; Aso *et al.*, 2010), while being inhibited by appetitive reinforcement signals (Cohn *et al.*, 2015). Similarly, the C3 cluster of honey bee projects diversely to mushroom bodies, suggesting its crucial role in regulating learning and memory. It contains ∼140 neurons per hemisphere (Tedjakumala *et al.*, 2017), which is remarkably greater than ∼25 in *Drosophila* (PPM3, PPL1, and PPL2ab combined together) (Mao & Davis, 2009) and ∼58 in pharaoh ant (PPM1/2/3, PPL1/2/3 combined together). In social Hymenoptera, including ants, the mushroom bodies are pronouncedly expanded compared to the solitary flies, accounting for ∼24% of all brain cells in pharaoh ant, compared to only ∼5% relative to all brain cells in flies (Li *et al.*, 2022; Liu & Li, 2024). Additionally, the Kenyon cell (KC) types in the ants are remarkably diversified compared to the flies (Sheng *et al.*, 2020; Li *et al.*, 2022; Liu & Li, 2024). Similarly, in honey bees, KCs have functionally diverged from their ancestral roles in sawflies, a basal solitary Hymenopteran species (Kuwabara *et al.*, 2023). The expansion of KCs is thought to be a preadaptation necessary for social living (Farris, 2016). Our findings that PPL1/3 neurons are significantly expanded in ants suggest that this group of neurons may have coevolved with a larger mushroom body to support advanced cognitive capabilities in social insects. Another cluster of dopamine neurons that is notably expanded in ants is the PAL neurons, which in flies project to lobula, optic tubercle, ventral medial protocerebrum, and superior posterior slope regions in the brain (Mao & Davis, 2009). However, the specific behavior regulated by PAL neurons, and whether this neuron group is involved in advanced social behaviors, remains to be elucidated.

Subset of dopamine neurons critical for reproductive division of labor

PPL2b appears to play a crucial role in regulating mating behaviors in ants, as it is present in gynes and males, which retain the ability to mate. In contrast, it is absent in workers and queens, which have permanently lost their mating capability. Our observation that PPL2b neurons, but not PPL2a neurons, are located immediately adjacent to *Nlg2*+ neurons suggest a potential anatomical connection. We therefore speculate that PPL2b neurons may relay visual information from *Nlg2*+ lobular neurons to the higher brain center, thereby promoting detection of courtship target and reproductive behaviors in gynes and males. In successfully mated queens, which no longer remate, this group of neurons appears to be lost through apoptotic cell death, whereas in workers, which are sterile and have permanently lost their reproductive capability, PPL2b neurons are entirely absent. However, due to technical limitations, such as the lack of genetic tools, we cannot directly confirm the specific role of PPL2b neurons in regulating reproductive behaviors in ants. Dopamine neurons are highly heterogenous and regulate a wide range of behaviors in ants (Barbero *et al.*, 2023). Current methods, such as pan-neuronal knockdown of *TH* expression via RNA interference, are insufficient to establish a causal relationship between PPL2b neurons and courtship regu-

lation. Identifying specific marker genes for PPL2b neurons will be crucial for uncovering their specific behavioral regulatory functions.

Single-cell transcriptomics may provide entry points to subdivide dopamine neurons

Although central brain dopamine neurons can be molecularly defined by *TH* expression and anatomically distinguished by the locations of their cell bodies, these neurons exhibit remarkable heterogeneity and play diverse roles in regulating a wide range of behaviors. To uncover their specific functions, it is crucial to finely subdivide dopamine neurons into distinct subsets. Indeed, in fruit flies, a repertoire of genetic driver lines has been developed to monitor and manipulate subsets of dopamine neurons (Liu *et al.*, 2012; Aso *et al.*, 2014; Kuo *et al.*, 2015; Xie *et al.*, 2018). Using these driver lines, studies have shown that small groups of dopamine neurons can profoundly influence specific behavioral performances, such as sleep, courtship, learning, and social space behaviors (Aso *et al.*, 2012; Liu *et al.*, 2012; 2014; Kuo *et al.*, 2015; Chen *et al.*, 2017; Xie *et al.*, 2018; Zhao *et al.*, 2018). Additionally, single-cell transcriptomics profiling has provided a comprehensive atlas of dopamine neurons in flies, revealing 24 transcriptionally distinct clusters (Ma *et al.*, 2023). Each cluster is uniquely defined by a set of preferentially expressed genes, including transcription factors, neuropeptides, G protein-coupled receptors, and cell surface molecules (Ma *et al.*, 2023). Using this as a reference, we identified multiple transcriptionally distinct dopamine neuron clusters and characterized specific marker genes to further subsubdivide these neurons. While genetic manipulation of specific subsets of dopamine neurons is currently beyond the reach of ant research, identifying the unique molecular signatures that define these subsets provides a foundation for future studies. This molecular characterization could serve as an entry point to explore how dopamine circuits are differentially assembled across ant castes and how these circuits contribute to the division of labor in the ant superorganism.

Hereby, we propose several potential investigative avenues. (1) By referring to the interactive partner relationship of the marker genes identified in the brain single-cell atlas, it is possible to infer the cellular connective networks between clusters of dopamine neurons and other brain cell types (Jin *et al.*, 2021). This approach would enable the examination of dynamics in dopamine neuronal communications that reflect caste- and age-related differentiations. (2) By investigating the outcome of knocking down coexpressed marker genes associated with specific dopamine neuron subsets, it may help elucidate the functional heterogeneity within dopamine populations. (3) The development of neuronal activity indicators in the research field of ant neurobiology is urgently needed. Such tools would allow for the identification of dopamine neurons activated in specific behavioral contexts through the colabeling of specific dopamine markers and these indicators.

Acknowledgments

This work was supported by the National Natural Science Foundation of China No. 32388102 to Guojie Zhang, No. 32170631 to Weiwei Liu and Yunnan Provincial Science and Technology Department, No. 202201AT070129, No. 202401BC070017 to Weiwei Liu. We would like to thank the Institutional Center for Shared Technologies and Facilities of Kunming Institute of Zoology (KIZ), Chinese Academy of Sciences (CAS) for providing us with confocal microscopy image acquisition. And we are grateful to Cong Li for his technical support. We thank Lin Xu from Key Laboratory of Animal Models and Human Disease Mechanisms, Kunming Institute of Zoology (KIZ), Chinese Academy of Sciences (CAS) for assistance with Imaris (Oxford Instruments) software.

Disclosure

All authors have seen and agree with the contents of the manuscript and there is no conflict of interest, including specific financial interest and relationships and affiliations relevant to the subject of manuscript.

References

Adel, M. and Griffith, L.C. (2021) The role of dopamine in associative learning in *Drosophila*: an updated unified model. *Neuroscience Bulletin*, 37, 831–852.

Arganda, S., Hoadley, A.P., Razdan, E.S., Muratore, I.B. and Traniello, J.F.A. (2020) The neuroplasticity of division of labor: worker polymorphism, compound eye structure and brain organization in the leafcutter ant *Atta cephalotes*. *Journal of Comparative Physiology A*, 206, 651–662.

Aso, Y., Hattori, D., Yu, Y., Johnston, R.M., Iyer, N.A., Ngo, T.T.B. *et al.* (2014) The neuronal architecture of the mushroom body provides a logic for associative learning. *eLife*, 3, e04577.

Aso, Y., Herb, A., Ogueta, M., Siwanowicz, I., Templier, T., Friedrich, A.B. *et al.* (2012) Three dopamine pathways in-

duce aversive odor memories with different stability. *PLoS Genetics*, 8, e1002768.

Aso, Y., Siwanowicz, I., Bräcker, L., Ito, K., Kitamoto, T. and Tanimoto, H. (2010) Specific dopaminergic neurons for the formation of labile aversive memory. *Current Biology*, 20, 1445–1451.

Baer, B. (2011) The copulation biology of ants (Hymenoptera: Formicidae). *Myrmecological News*, 14, 55–68.

Barbero, F., Mannino, G. and Casacci, L.P. (2023) The role of biogenic amines in social insects: with a special focus on ants. *Insects*, 14, 386.

Beaulieu, J.M. and Gainetdinov, R.R. (2011) The physiology, signaling, and pharmacology of dopamine receptors. *Pharmacological Reviews*, 63, 182–217.

Blenau, W. and Baumann, A. (2001) Molecular and pharmacological properties of insect biogenic amine receptors: lessons from *Drosophila melanogaster* and *Apis mellifera*. *Archives of Insect Biochemistry and Physiology*, 48, 13–38.

Bonasio, R., Zhang, G., Ye, C., Mutti, N.S., Fang, X., Qin, N. *et al.* (2010) Genomic comparison of the ants *Camponotus floridanus* and *Harpegnathos saltator*. *Science*, 329, 1068–1071.

Boulay, R., Hooper-Bùi, L.M. and Woodring, J. (2001) Oviposition and oogenesis in virgin fire ant females *Solenopsis invicta* are associated with a high level of dopamine in the brain. *Physiological Entomology*, 26, 294–299.

Chandra, V., Fetter-Pruneda, I., Oxley, P.R., Ritger, A.L., McKenzie, S.K., Libbrecht, R. *et al.* (2018) Social regulation of insulin signaling and the evolution of eusociality in ants. *Science*, 361, 398–402.

Chen, J., Guan, Z., Sun, L., Fan, X., Wang, D., Yu, X. *et al.* (2024) N-methyladenosine modification of RNA controls dopamine synthesis to influence labour division in ants. *Molecular Ecology*, 33, e17322.

Chen, S.L., Chen, Y.H., Wang, C.C., Yu, Y.W., Tsai, Y.C., Hsu, H.W. *et al.* (2017) Active and passive sexual roles that arise in *Drosophila* male-male courtship are modulated by dopamine levels in PPL2ab neurons. *Scientific Reports*, 7, 44595.

Claridge-Chang, A., Roorda, R.D., Vrontou, E., Sjulson, L., Li, H., Hirsh, J. *et al.* (2009) Writing memories with light-addressable reinforcement circuitry. *Cell*, 139, 405–415.

Cohn, R., Morantte, I. and Ruta, V. (2015) Coordinated and compartmentalized neuromodulation shapes sensory processing in *Drosophila*. *Cell*, 163, 1742–1755.

Farris, S.M. (2016) Insect societies and the social brain. *Current Opinion in Insect Science*, 15, 1–8.

Fleming, S.J., Marioni, J.C. and Babadi, M. (2019) CellBender remove-background: a deep generative model for unsupervised removal of background noise from scRNA-seq datasets. *BioRxiv*, 791699.

Friedman, D.A., Pilko, A., Skowronska-Krawczyk, D., Krasinska, K., Parker, J.W., Hirsh, J. *et al.* (2018) The role of dopamine in the collective regulation of foraging in Harvester Ants. *iScience*, 8, 283–294.

Gao, Q., Xiong, Z., Larsen, R.S., Zhou, L., Zhao, J., Ding, G. *et al.* (2020) High-quality chromosome-level genome assembly and full-length transcriptome analysis of the pharaoh ant *Monomorium pharaonis*. *GigaScience*, 9, giaa143.

Giraldo, Y.M., Patel, E., Gronenberg, W. and Traniello, J.F. (2013) Division of labor and structural plasticity in an extrinsic serotonergic mushroom body neuron in the ant *Pheidole dentata*. *Neuroscience Letters*, 534, 107–111.

Goolsby, B.C., Smith, E.J., Muratore, I.B., Coto, Z.N., Muscedere, M.L. and Traniello, J.F.A. (2024) Differential neuroanatomical, neurochemical, and behavioral impacts of early-age isolation in a eusocial insect. *Brain, Behavior and Evolution*, 99, 171–183.

Gordon, D.G., Zelaya, A., Arganda-Carreras, I., Arganda, S. and Traniello, J.F.A. (2019) Division of labor and brain evolution in insect societies: neurobiology of extreme specialization in the turtle ant *Cephalotes varians*. *PLoS ONE*, 14, e0213618.

Gospocic, J., Shields, E.J., Glastad, K.M., Lin, Y., Penick, C.A., Yan, H. *et al.* (2017) The neuropeptide corazonin controls social behavior and caste identity in ants. *Cell*, 170, 748–759.e12.

Greer, C.L., Grygoruk, A., Patton, D.E., Ley, B., Romero-Calderon, R., Chang, H.Y. *et al.* (2005) A splice variant of the *Drosophila* vesicular monoamine transporter contains a conserved trafficking domain and functions in the storage of dopamine, serotonin, and octopamine. *Journal of Neurobiology*, 64, 239–258.

Hölldobler, B. and Wilson, E.O. (1990) *The ants*. Harvard University Press.

Jin, S., Guerrero-Juarez, C.F., Zhang, L., Chang, I., Ramos, R., Kuan, C.H. *et al.* (2021) Inference and analysis of cell-cell communication using CellChat. *Nature Communications*, 12, 1088.

Kamhi, J.F., Nunn, K., Robson, S.K.A. and Traniello, J.F.A. (2015) Polymorphism and division of labour in a socially complex ant: neuromodulation of aggression in the Australian weaver ant, *Oecophylla smaragdina*. *Proceedings of The Royal Society B-Biological Sciences*, 282, 20150704.

Kuo, S.Y., Wu, C.L., Hsieh, M.Y., Lin, C.T., Wen, R.K., Chen, L.C. *et al.* (2015) PPL2ab neurons restore sexual responses in aged *Drosophila* males through dopamine. *Nature Communications*, 6, 7490.

Kuwabara, T., Kohno, H., Hatakeyama, M. and Kubo, T. (2023) Evolutionary dynamics of mushroom body Kenyon cell types in hymenopteran brains from multifunctional type to functionally specialized types. *Science Advances*, 9, eadd4201.

Li, Q., Wang, M., Zhang, P., Liu, Y., Guo, Q., Zhu, Y. *et al.* (2022) A single-cell transcriptomic atlas tracking the neural basis of division of labour in an ant superorganism. *Nature Ecology & Evolution*, 6, 1191–1204.

Li, R., Dai, X., Zheng, J., Larsen, R.S., Qi, Y., Zhang, X. *et al.* (2024) Juvenile hormone as a key regulator for asymmetric caste differentiation in ants. *Proceedings of the National Academy of Sciences USA*, 121, e2406999121.

Libbrecht, R., Oxley, P.R. and Kronauer, D.J.C. (2018) Clonal raider ant brain transcriptomics identifies candidate molecular mechanisms for reproductive division of labor. *BMC Biology*, 16, 89.

Liu, Q., Liu, S., Kodama, L., Driscoll, M.R. and Wu, M.N. (2012) Two dopaminergic neurons signal to the dorsal fan-shaped body to promote wakefulness in *Drosophila*. *Current Biology*, 22, 2114–2123.

Liu, W. and Li, Q. (2024) Single-cell transcriptomics dissecting the development and evolution of nervous system in insects. *Current Opinion in Insect Science*, 63, 101201.

Ma, D., Herndon, N., Le, J.Q., Abruzzi, K.C., Zinn, K. and Rosbash, M. (2023) Neural connectivity molecules best identify the heterogeneous clock and dopaminergic cell types in the *Drosophila* adult brain. *Science Advances*, 9, eade 8500.

Mannino, G., Abdi, G., Maffei, M.E. and Barbero, F. (2018) Origanum vulgare terpenoids modulate *Myrmica scabrinodis* brain biogenic amines and ant behaviour. *PLoS ONE*, 13, e0209047.

Mannino, G., Casacci, L.P., Bianco Dolino, G., Badolato, G., Maffei, M.E. and Barbero, F. (2023) The geomagnetic field (GMF) is necessary for black garden ant (*Lasius niger* L.) foraging and modulates orientation potentially through aminergic regulation and *MagR* expression. *International Journal of Molecular Sciences*, 24, 4387.

Mao, Z. and Davis, R.L. (2009) Eight different types of dopaminergic neurons innervate the *Drosophila* mushroom body neuropil: anatomical and physiological heterogeneity. *Frontiers in Neural Circuits*, 3, 5.

Muratore, I.B., Fandozzi, E.M. and Traniello, J.F.A. (2022) Behavioral performance and division of labor influence brain mosaicism in the leafcutter ant *Atta cephalotes*. *Journal of Comparative Physiology A*, 208, 325–344.

Muscedere, M.L. and Traniello, J.F.A. (2012) Division of labor in the hyperdiverse ant genus *Pheidole* is associated with distinct subcaste- and age-related patterns of worker brain organization. *PLoS ONE*, 7, e31618.

Mustard, J.A., Beggs, K.T. and Mercer, A.R. (2005) Molecular biology of the invertebrate dopamine receptors. *Archives of Insect Biochemistry and Physiology*, 59, 103–117.

Nässel, D.R. and Elekes, K. (1992) Aminergic neurons in the brain of blowflies and *Drosophila*: dopamine- and tyrosine hydroxylase-immunoreactive neurons and their relationship with putative histaminergic neurons. *Cell and Tissue Research*, 267, 147–167.

Okada, Y., Sasaki, K., Miyazaki, S., Shimoji, H., Tsuji, K. and Miura, T. (2015) Social dominance and reproductive differentiation mediated by dopaminergic signaling in a queenless ant. *Journal of Experimental Biology*, 218, 1091–1098.

Opachaloemphan, C., Yan, H., Leibholz, A., Desplan, C. and Reinberg, D. (2018) Recent advances in behavioral (epi)genetics in eusocial insects. *Annual Review of Genetics*, 52, 489–510.

Qiu, B., Dai, X., Li, P., Larsen, R.S., Li, R., Price, A.L. *et al.* (2022) Canalized gene expression during development mediates caste differentiation in ants. *Nature Ecology & Evolution*, 6, 1753–1765.

Qiu, B., Larsen, R.S., Chang, N.C., Wang, J., Boomsma, J.J. and Zhang, G. (2018) Towards reconstructing the ancestral brain gene-network regulating caste differentiation in ants. *Nature Ecology & Evolution*, 2, 1782–1791.

Rajakumar, R., Koch, S., Couture, M., Favé, M.-J., Lillico-Ouachour, A., Chen, T. *et al.* (2018) Social regulation of a rudimentary organ generates complex worker-caste systems in ants. *Nature*, 562, 574–577.

Ribeiro, I.M.A., Drews, M., Bahl, A., Machacek, C., Borst, A. and Dickson, B.J. (2018) Visual projection neurons mediating directed courtship in *Drosophila*. *Cell*, 174, 607–621.e18.

Schnell, B., Raghu, S.V., Nern, A. and Borst, A. (2012) Columnar cells necessary for motion responses of wide-field visual interneurons in *Drosophila*. *Journal of Comparative Physiology A*, 198, 389–395.

Schwander, T., Humbert, J.Y., Brent, C.S., Cahan, S.H., Chapuis, L., Renai, E. *et al.* (2008) Maternal effect on female caste determination in a social insect. *Current Biology*, 18, 265–269.

Sheng, L., Shields, E.J., Gospocic, J., Glastad, K.M., Ratchasanmuang, P., Berger, S.L. *et al.* (2020) Social reprogramming in ants induces longevity-associated glia remodeling. *Science Advances*, 6, eaba9869.

Simola, D.F., Graham, R.J., Brady, C.M., Enzmann, B.L., Desplan, C., Ray, A. *et al.* (2016) Epigenetic (re)programming of caste-specific behavior in the ant *Camponotus floridanus*. *Science*, 351, aac6633.

Smith, A.R., Muscedere, M.L., Seid, M.A., Traniello, J.F.A. and Hughes, W.O.H. (2013) Biogenic amines are associated with worker task but not patriline in the leaf-cutting ant *Acromyrmex echinatior*. *Journal of Comparative Physiology A*, 199, 1117–1127.

Szathmáry, E. and Smith, J.M. (1995) The major evolutionary transitions. *Nature*, 374, 227–232.

Tedjakumala, S.R., Rouquette, J., Boizeau, M.L., Mesce, K.A., Hotier, L., Massou, I. *et al.* (2017) A tyrosine-hydroxylase characterization of dopaminergic neurons in the honey bee brain. *Frontiers in Systems Neuroscience*, 11, 47.

Wada-Katsumata, A., Yamaoka, R. and Aonuma, H. (2011) Social interactions influence dopamine and octopamine homeostasis in the brain of the ant *Formica japonica*. *Journal of Experimental Biology*, 214, 1707–1713.

Wheeler, W.M. (1910) Ants. Their structure, development and behavior. *Science*, 31, 860–862.

Wheeler, W.M. (1911) The ant-colony as an organism. *Journal of Morphology*, 22, 307–326.

Wissink, M. and Nehring, V. (2021) Appetitive olfactory learning suffers in ants when octopamine or dopamine receptors are blocked. *The Journal of Experimental Biology*, 224, jeb242732.

Xie, T., Ho, M.C.W., Liu, Q., Horiuchi, W., Lin, C.C., Task, D. *et al.* (2018) A genetic toolkit for dissecting dopamine circuit function in *Drosophila*. *Cell Reports*, 23, 652–665.

Yaffe, D., Forrest, L.R. and Schuldiner, S. (2018) The ins and outs of vesicular monoamine transporters. *Journal of General Physiology*, 150, 671–682.

Yamamoto, S. and Seto, E.S. (2014) Dopamine dynamics and signaling in *Drosophila*: an overview of genes, drugs and behavioral paradigms. *Experimental Animals*, 63, 107–119.

Zhao, X., Lenek, D., Dag, U., Dickson, B.J. and Keleman, K. (2018) Persistent activity in a recurrent circuit underlies courtship memory in *Drosophila*. *eLife*, 7, e31425.

Manuscript received December 25, 2024
Final version received May 6, 2025
Accepted May 6, 2025

Supporting Information

Additional supporting information may be found online in the Supporting Information section at the end of the article.

Extended Materials and methods

Table S1 Numbers of dopamine immunoreactive neurons found in the brain and their distributions across 4 castes.

Table S2 The sequence of hybridization chain reaction (HCR) RNA *in situ* hybridization probe sets.

Table S3 Marker gene list of monoaminergic transcriptional clusters in *Monomorium pharaonis* brains.

Table S4 Enriched Gene Ontology (GO) terms of dopamine transcriptional clusters in *Monomorium pharaonis*.

Fig. S1 Heatmap of marker gene expression in dopamine transcriptional clusters. Heatmaps showing the expression levels of neuropeptides, GPCRs (G protein-coupled receptors) and CSMs (cell surface molecules) in specific dopaminergic neuron clusters.

Fig. S2 Validation of neuropeptide gene expression in specific dopaminergic clusters of pharaoh ant. Costaining of neuropeptide genes *CAPA*, *Dh31*, *TK* and *Nplp1* (green) respectively with *ple* (red) by hybridization chain reaction (HCR) probes. The dotted white box indicates the co-stained neurons found from anterior and posterior views. The table summarizes the specific dopamine clusters that express the particular neuropeptides.

Fig. S3 Uniform dopamine neuron clusters across ant castes. (A–D) PAM1/2 in ant brain from the anterior view. (E–H) SVP and VUM1/2 in subesophageal zone (SEZ) from the posterior view. (I–L) Box plot showing the cell number per hemisphere of the uniform dopamine clusters (one-way analysis of variance followed by Newman-Keuls Multiple Comparison test). Blue in A–H indicates 4′,6-diamidino-2-phenylindole; green indicates nc82; magenta indicates dopamine neuron cell body detected by immuno-histochemistry. The brain orientation is indicated: A = anterior, P = posterior, D = dorsal, V = ventral L = left, R = right.